# Finite Element Analysis of Switched Reluctance Generator under Fault Condition Oriented Towards Diagnosis of Eccentricity Fault

**Ebrahim Afjei and Hossein Torkaman**

Department of Electrical and Computer Engineering
Shahid Beheshti University, G.C., Tehran, Iran
E-Afjei@sbu.ac.ir; H_Torkaman@sbu.ac.ir

*Abstract* ─ In this paper, a novel two phase double layer switched reluctance generator (DLSRG) under static eccentricity fault is introduced and analyzed. The proposed generator consists of two magnetically independent stator and rotor layers. There is a stationary reel, which has the field coils wrapped around it and is placed between the two-stator sets. This paper then continues with modeling this generator in the field assisted mode for healthy condition as well as motor with static rotor eccentricity utilizing three-dimensional finite element analysis (3-D FEA). The results of the numerical analysis for a (4/2)×2 DLSRG including flux linkages, mutual inductances per phase in each layer and radial force for various eccentric generator conditions by considering the end effects and axial fringing fields for simulating reliable model are obtained and compared. Consequently, Fourier analysis is carried out to study the variations of mutual inductance as a diagnosis index. The obtained results present useful information as good candidates for fault indicators as well as the amount of eccentricity fault and the direction of fault occurrence.

*Index Terms* ─ Eccentricity, fault diagnosis, switched reluctance generator (SRG), 3-D finite element method.

## I. INTRODUCTION

Switched reluctance generators (SRG) have been gradually engaged in variable-speed applications due to its fundamental advantages of low manufacturing cost, simple and rigid structure, easiness of maintenance, excellent speed regulation, simple converter circuit, no rotor windings or permanent magnet, and easy cooling feature, etc [1-3]. The SRG has been proved as a good alternative for some applications like wind turbine generator, battery charger, and as an alternator for automotive applications [4-6].

On the other side, one of the most common types of fault in electrical machines is the eccentricity fault. Eccentricity exists in a machine when there is an uneven air gap between the stator and the rotor [7, 8]. Static eccentricity is caused by different factors such as, weight of the rotor/load or interconnecting rotor belt. The end result can cause electrically induced vibration that reduces the life of bearings and also increases the potential for stator/ rotor rubbing and damages to the insulation systems.

The effect of eccentricity fault on the torque profile of an SR motor with 2-D FEM has been considered in [9] and the result shows the static torque does not change much with relative eccentricity up to 50%. It is also shown with an increase in the eccentricity; there will be an increase in the fundamental, 8th, 10th, 14th, and 15th torque components. In [10], it is shown that with the increase in eccentricity, the average overall torque increases along with an increase in all of ripple contents. Dorrell *et al*. in [11] have investigated the effect of eccentricity on torque profile with respect to the switching angle. A method is presented in [12] for computing the radial magnetic forces in SR motor which includes iron saturation and eccentricity. Also, the unbalanced forces were evaluated using three different methods, namely static 2-D FEM, an analytical model, and a simplified analytical model. In [13], a dynamic response of motor under static and dynamic eccentricities has been studied using coupled 2-D FE in Matlab environment.

In the previous works, the authors have analyzed the SRG [14, 15] and SRM [16] under healthy mode utilizing 2-D and 3-D FEM. In [17], [7], and [18], the static, dynamic, and mixed eccentricity faults in the SRM are considered, respectively. Afterward, the intervals for different modes of motor operations (normal and faulty) are calculated by hybrid method in [8]. In this paper, static eccentricity in SRG is considered, for the new generator configuration.

The eccentricity fault has been studied in other generators and different applications such as [19-21], while almost there is no literature for considering the effects of eccentric rotor on the performance of SRG. This paper is an attempt to achieve this purpose.

This paper is organized as follows: the DLSRG modeling and geometrical parameters of implemented generator are presented in Section II. Section III discusses the definition of static eccentricity in generator operation. In Section IV, the finite element results of the generator profiles under normal and eccentricity fault are obtained and discussed. Results of harmonic components analysis utilizing fast Fourier transform for various eccentricities are presented in Section V. Consequently, some concluding remarks are provided in Section VI.

## II. FINITE ELEMENT MODELING OF DLSRG

Accurate modeling of electrical systems is necessary in performance prediction and verification of the systems, hence to evaluate properly the generator performance a reliable model is required. The finite element method can be one of the best choices for the providing precise model for such a purpose. Therefore, a three dimensional finite element analysis is being used to determine the magnetic field distribution in and around the generator. In order to present the operation of the motor and to determine the main machine profiles at different rotor positions, the field solutions are obtained.

It has been shown that the 3-D FE approach is a precise and realistic method in comparison with the 2-D FE approach from the results obtained by the authors in [16]. The variations between 3-D/2-D FE results are due to the consideration of the end effects and also the axial fringing field in 3-D FE analysis.

The field analysis has been performed based on the variational energy minimization technique to solve for the electric vector potential. In this method, electric vector potential known as $T - \Omega$ formulation was explained by authors in [8].

The proposed generator for this study consists of two magnetically dependent stator and rotor sets (layers). The two layers are exactly symmetrical with respect to a plane perpendicular to the middle of the motor shaft. Where each stator set includes four salient poles having 45º arc length with windings wrapped around them (Fig. 1a) while, the rotor comprises of two salient poles that have different arc lengths (Fig. 1b) without any windings. The arc of each rotor pole is the same as stator pole (45º) in one side and twice as much in the other side. The side view of complete generator assembly is depicted in Fig. 1c.

There is a stationary reel, which has the field coils wrapped around it and is placed between the two-stator sets over the rotor shaft which is named as an assisted field. The motor shaft passes through a hole in the middle of the stationary reel and acts as a core for the field coil assembly.

In this format, the developed magnetic field produced by the field travels from the motor shaft to the rotor then to the stator assembly and finally completes its path via the generator housing. The cut view of the generator system with the flux path is depicted in Fig. 2 that will be analyzed using the three dimensional finite elements.

The proposed DLSR generator dimensions are listed in Table I.

The significant features in the new configuration of SR generator that make it distinct from other types of SRG are: a) the new DLSRG consist of two layers to produce South poles in one layer and the North Pole in the other layer; b) the new rotor comprises of two salient poles with different arc lengths. The rotor is shaped in such a way to produce starting torque as well as having rising inductance in all of 90º rotor arc length; c) existence of a field assisted coil on the stationary reel between two layers produces an independent field; d) due to existence of assisted field, this generator can produce higher output power than a standard self excited SRG.

It has been assumed that each analysis is carried out with four-node tetrahedral blocks for the present study.

a)



b)



c)
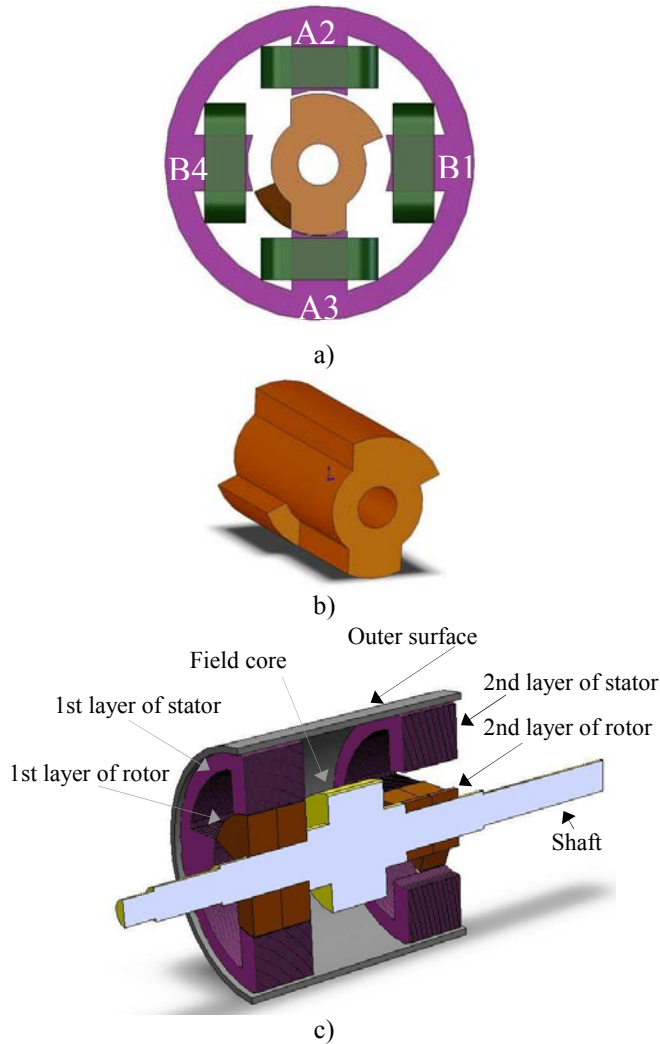
Fig. 1. a) Front view of 1st layer in DLSRG, b) rotor shape, c) a side view of DLSRG assembly (without coils).
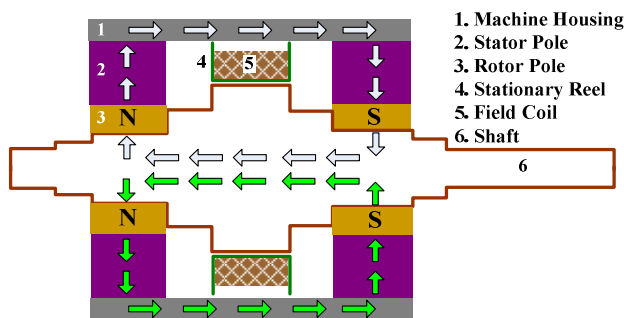


Fig. 2. A cut view of DLSRG with the flux path.

The schematic figure showing the meshes in the simulation study is illustrated in Fig. 3. In this analysis, the usual assumptions such as the magnetic field outside of an air box in which the

generator is placed, is considered to be zero. Also, the analysis includes a 360 degree rotation of the rotor for the analysis of SRG behavior at the different rotor positions. Due to symmetrical behavior of the field in and around the generator, only the rotor movement of the 1st layer from unaligned to unaligned position is considered. The rotor of 2nd layer moves from fully unaligned to fully aligned position as well; therefore, all machine parameters for these points and the points in between can be computed. In this study, assisted field winding consists of 300 turns with a current magnitude of 0.5 A.

Layer one of the machine includes coils 1, 2, 3, and 4 in which coils 2, 3 belong to phase A, and coils 1, 4 belong to phase B. In layer two coils 5, 7 belong to phase A, and coils 6, 8 belong to phase B.

Table 1: DLSR generator dimensions

| Parameter | Value |
|---|---|
| Stator core outer diameter | 72mm |
| Stator core inner diameter | 62mm |
| Stator arc | 45deg |
| Air gap | 0.25mm |
| Rotor core outer diameter | 39.5mm |
| Rotor shaft diameter | 10mm |
| Rotor larger arc | 90deg |
| Rotor smaller arc | 45deg |
| Stack length | 35mm |
| Number of turns per pole | 110 |
| Number of turns for field coil | 300 |
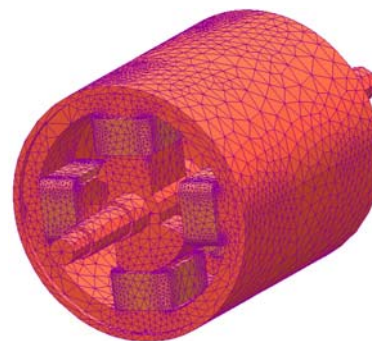


Fig. 3. Finite element mesh for the DLSRG.

## III. STATIC ECCENTRICITY DEFINITION

In this type of eccentricity, the air gap distribution around the rotor is not uniform, and is

time-independent. It occurs when the rotational axis of the rotor is identical to its symmetrical axis but has been displayed with respect to the stator symmetrical axis. The degree of static eccentricity or relative eccentricity is defined as follows

$$\varepsilon_S = \left(\frac{r}{g}\right) \times 100 \ (\%), \qquad (1)$$

where, $\varepsilon_S$ is the percentage eccentricity between the stator and rotor axes, $g$ is the radial air gap length in the case of uniform air gap in healthy generator or with no eccentricity, and $r$ is the displacement of the rotor in the horizontal direction to the excited stator poles in aligned position.

Manufacturers normally keep the total eccentricity level as low as possible in order to minimize unbalanced magnetic pull (UMP) as well as the reduction of vibration and noise. An air gap eccentricity of up to 10% is permissible as mentioned in the references. Also, due to the collision of the rotor pole with the stator pole, the relative eccentricity of more than 60% is not considered in this study.

## IV. NUMERICAL RESULTS AND ANALYSIS OF DLSRG UNDER ECCENTRIC CONDITION

The reluctance variation of the generator has an important role on the performance; hence, an accurate knowledge of the flux distribution inside the generator for different excitation currents and rotor positions are essential for the prediction of machine performance.

In order to evaluate these characteristics and also investigate the effects of static eccentricity on the two-phase switched reluctance generator behavior, the generator is simulated utilizing the 3-D finite element analysis. In this analysis, the static eccentricity fault is considered in phase A direction. Hence, the rotor pole is closer to coil 3 and further away from coil 2.

### A. Influence of eccentricity upon DLSR generator radial force

The eccentricity fault leads to a radial force on the rotor which tries to pull it even further away from the stator bore center. On the other hand, this phenomenon causes an unbalanced

electromagnetic force in the generator. Figure 4 shows the normal radial force exerted on the rotor poles from unaligned to fully aligned and then to unaligned positions for different eccentricities.
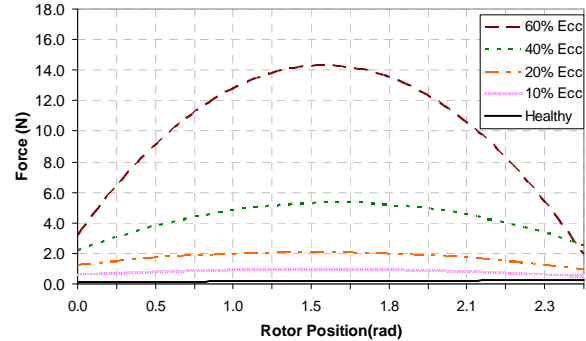


Fig. 4. Radial force in pole 2 from phase A in field assisted mode.

As shown in Fig. 4, the radial force is almost zero in healthy mode due to the magnetic pull compensation of the opposite poles.

Figure 4 shows about 140 times larger radial force when 60% eccentricities are occurred in comparison with healthy mode. Also, the radial force has increased by a factor of 3 when the eccentricity has changed from 40% to 60%. It has also been shown that, the maximum force is produced when the rotor poles are fully aligned with the stator poles. It is also evident from the figure, when the amount of eccentricity fault increases, the exerted force will also go up as well.

### B. Influence of eccentricity upon DLSR generator mutual flux

In the field assisted mode of operation, the stationary reel that is placed between the two-stator layers is set at 0.6A, and the stator coils are not excited. In this format, the developed magnetic field from the stator poles travels to the rotor then to the shaft and finally completes its path via the generator housing. In this mode of operation, the power generation is obtained by energizing the proper stator coils during the negative inductance periods. Therefore, the flux linkage of phase A and B are calculated from unaligned to fully aligned and then to unaligned positions (the fully aligned position is at 1.57 radian). Regarding to the occurrence of fault in direction of phase A, the variations of flux in coils 1 and 4 from phase B are

negligible, while, the variation of flux in coils 2,3 of phase A are noticeable, Fig. 5 and Fig. 6 show the flux variations for a healthy generator and a generator with various eccentricities. In these figures, the flux data points have been estimated with second order functions using least squares method, for better illustration.

The non-uniformity of air gap is time invariant when static eccentricity exists; therefore, the distribution of air gap does not change as the rotor turns. Hence, the flux for each phase is repeated identically in every cycle.
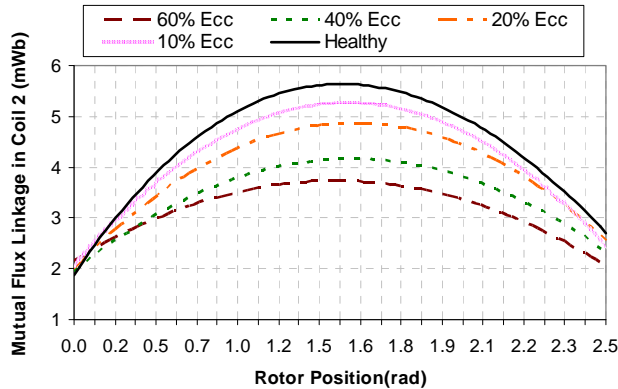


Fig. 5. Mutual flux linkage in coil 2 from phase A in field assisted mode.
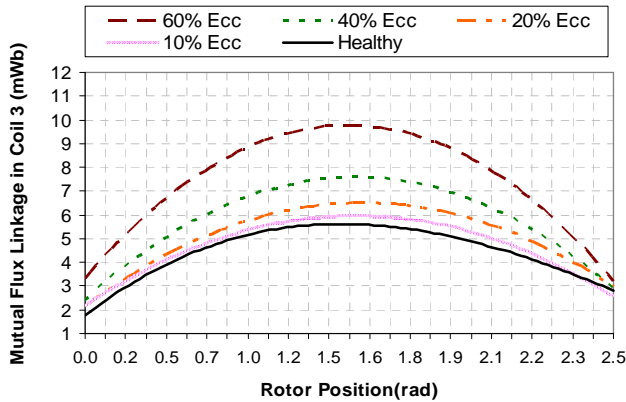


Fig. 6. Mutual flux linkage in coil 3 from phase A in field assisted mode.

## C. Influence of eccentricity upon DLSR generator mutual inductance

It is imperative to look at the field coil inductance curve at this point to see how it varies as the rotor turns. It can provide useful information for explaining the influence of fault in generator operation.

The so called "effective" mutual inductance has been defined as the ratio of each phase flux linkages to the exciting current of assistant field ($\lambda(\theta)/I_f$). Based on this definition, the mutual inductance value of coil 2 in phase A versus rotor position is presented in Fig. 7 for healthy motor as well as the motor with a range of eccentricity faults. In Fig. 7, the shape of mutual inductance from aligned position to unaligned position (1.57 rad-2.5 rad) is depicted and also linear approximation is utilized for more accuracy and clarity.
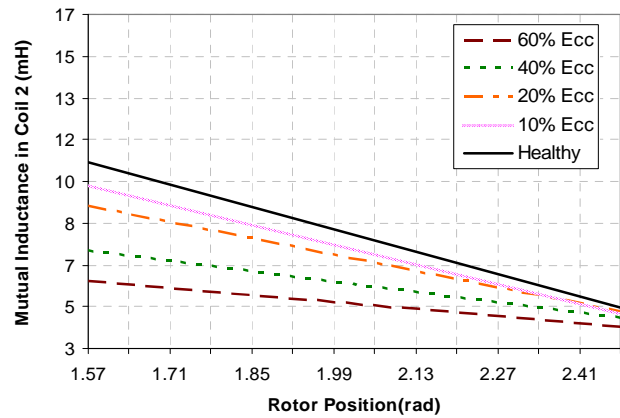


Fig. 7. Mutual inductance in coil 2 from phase A in field assisted mode.

As seen from curves in Fig. 7, the slopes of mutual inductance decrease when the eccentricity levels go up, and also the magnitudes of mutual inductance for each eccentricity level reduces, as the rotor move into the unaligned position. It is also observed that amplitude of mutual inductance of the A-2 has 45%, 32%, 18%, and 9% reduction with 60%, 40%, 20%, and 10% eccentricities compared with healthy generator in fully aligned position, respectively as shown in Fig. 7. Also, as shown in this figure, the slopes of mutual inductance in A-2 for 60%, 40%, 20%, and 10% fault is about 2.2, 1.8, 1.3, and 0.5 times lower than the slope of mutual inductance in a healthy generator.

These reductions are due to air gap length increases between the stator and rotor poles in front of coil 2. On the other hand, the eccentricity phenomenon caused to reduce the difference between maximum and minimum mutual

inductance values in coil 2. Since the produced torque and induced voltage in SR machines are directly proportional to the variation of inductance with respect to rotor position, then the torque and voltage production profiles in motoring and generating modes of operation will vary accordingly. The following formulas for the SR machine in the linear mode of operation will prove the above statement.

$$T = \frac{1}{2}i^2\frac{dL}{d\theta} \qquad (2)$$

$$e_{ind} = \omega\frac{d\lambda}{d\theta} \qquad (3)$$

where, $T$ is the torque, $i$ is phase current, $L$ is phase inductance, $\theta$ is rotor position, $e_{ind}$ is generated voltage and $\omega$ is angular speed.

Figure 8 shows the calculated mutual inductance versus rotor position obtained by the ratio of flux linking coil 3 to the field current.

As depicted in this figure, the magnitude of mutual inductance has been increased, for each rotor position. As the eccentricity levels go up, the slope of mutual inductance will also change noticeably. The slopes of mutual inductance in A-3 for eccentric generator under 60%, 40%, 20%, and 10% fault has almost 47%, 36%, 16%, and 8% higher value than the slope of mutual inductance in a healthy generator.
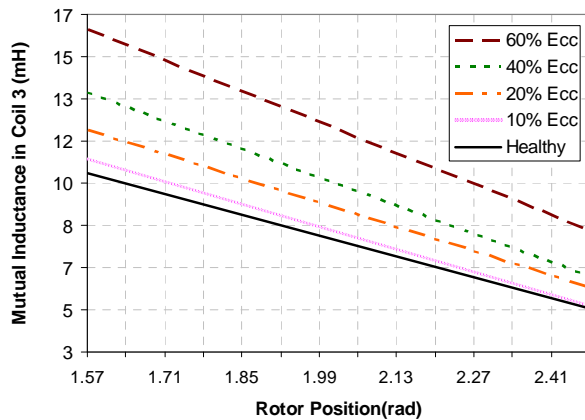


Fig. 8. Mutual inductance in coil 3 from phase A in field assisted mode.

Also, as demonstrated in this figure, amplitude of mutual inductance of the A-3 has 56%, 28%, 16%, and 4.8% increase with 60%, 40%, 20%, and 10% eccentricity compared with a healthy generator in the fully aligned position, respectively

as shown in Fig. 8. These changes are due to the decrease in the air gap length between the stator and rotor poles in front of coil 3.

Therefore, variation of mutual inductances, as well as the area under their curves can be addressed as a fine index for eccentricities diagnosis.

The mutual inductance in other coils such as 1, 4 do not experience noticeable changes. The calculated results and the shape of mutual inductance in Fig. 7 and Fig. 8 point to two fundamental achievements: first, the variations of each coil and its magnitude present the fault occurrence and the level of eccentricity. Second, the increased mutual inductance magnitude of coil 2 and the reduction of mutual inductance magnitude of coil 3 shows that the rotor pole is near coil 3 and further away from coil 2, therefore the direction of fault can also be detected in this manner.

## V. Fourier Analysis of Mutual Inductance/Rotor Angular Position Characteristics

The fast Fourier transform (FFT) is a classical spectral estimation technique which is an efficient algorithm and one of the most robust ones. Therefore, the analysis based on FFT has been proposed to extract frequency information from the mutual inductance as a diagnostic index in order to detect the rotor misplacement.

Results of the harmonic components analysis for the mutual inductance profile in phase A (faulty phase) in the field assisted mode using 3-D FEM for various eccentricities are presented in Fig. 9 and Fig. 10. As depicted in Fig. 9 with an increase in the eccentricity level, there is a decrease in the fundamental harmonic and other components of mutual inductances in coil 2. These changes obtained from the mutual inductance curve behavior in time domain. As shown in this figure, the amplitude of the fundamental component in coil 2 for healthy motor is almost 1.5 times higher than those of fundamental components in a faulty motor with 60% eccentricity. Also, in eccentric motor with 10%, 20%, and 40% faults, these components are faced with 7%, 12%, and 25% drop in their amplitudes. It is observed that variations of other components are also the same as the fundamental component.

Figure 10 illustrates that the fundamental harmonic as well as other harmonic components of mutual inductance in coil 3 have increased with raising the eccentricity level. These changes are due to reduction of the corresponding air gap size in the time domain, which affects the amplitude of the frequency components. As shown in this figure, the amplitude of fundamental component in coil 3 for faulty generator with 60% eccentricity is almost 1.5 times higher than those of fundamental component in a healthy motor. In addition, this component experiences 4.5%, 16.7%, and 29.6% rise in its magnitude in eccentric motor with 10%, 20%, and 40% faults. It is also observed that the variations of other frequency components are the same as the fundamental component.

higher than the slope of mutual inductance in a healthy generator.

The amplitude and slope of mutual inductance in time domain and its amplitude of a fundamental component in frequency domain were used for fault diagnosis and then proposed as a diagnostic index. Regarding to the fault detection in DLSRG, useful results can be obtained by just evaluating only one of the phases from each layer, moreover this procedure and diagnosis can be applied to other types of SRG as well. On the other side, the calculated results show that the direction of static eccentricity fault can be effectively detected by evaluation of this index from two coils in one phase.



Fig. 9. FFT of mutual inductance in coil 2 from phase A for 3-D FEM in healthy motor and motor with various eccentricities.
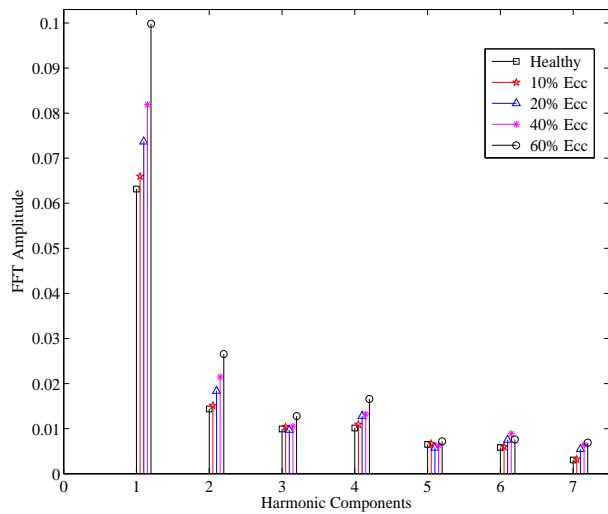


Fig. 10. FFT of mutual inductance in coil 3 from phase A for 3-D FEM in healthy motor and motor with various eccentricities.

## VI. CONCLUSION

This paper analyzes the eccentricity fault diagnosis in a new two phase switched reluctance generator. For this purpose, the static eccentricity was modeled and analyzed using 3-D-FEM by considering the end effects and axial fringing fields for implementation of a reliable model. With occurrence of fault, it is observed that the amplitude of mutual inductance of coils 2 and 3 from faulty phase (A) with 60% eccentricity will show 45% reduction and 56% increase compared with a healthy generator in the fully aligned position. Also, the slopes of the mutual inductance in coils 2 and 3 from faulty phase (A) for 60% fault are about 2.2 times lower and 0.47 times

## ACKNOWLEDGMENT

## REFERENCES

[1] Y. Chang, and C. Liaw, "On the Design of Power Circuit and Control Scheme for Switched Reluctance Generator," *IEEE Transactions on Power Electronics,* vol. 23, no. 1, pp. 445-454, 2008.

[2] E. Afjei, and H. Torkaman, "Comparison of Two Types of Dual Layer Generator in Field Assisted Mode Utilizing 3-D-FEM and Experimental Verification," *Progress in*

*Electromagnetics Research B,* vol. 23, pp. 293-309, 2010.

[3] D. Torrey, "Switched Reluctance Generators and Their Control," *IEEE Transaction on Industrial Electronic,* vol. 49, no. 1, pp. 3-14, 2002.

[4] D. McSwiggan, L. Xu, and T. Littler, "Modelling and Control of a Variable Speed Switched Reluctance Generator based Wind Turbine," in 42nd International Universities Power Engineering Conference, pp. 459-463, 2007.

[5] L. Moreau, M. Machmoum, and M. E. Zaïm, "Design of Low-Speed Slotted Switched Reluctance Machine for Wind Energy Applications," *Electric Power Components and Systems, Taylor and Francis,* vol. 34, no. 10, pp. 1139-1156, 2006.

[6] A. Martinez, and *et al.*, "Use of an AC Self-Excited Switched Reluctance Generator as a Battery Charger," in 13th Power Electronics and Motion Control Conference, pp. 845–849, 2008.

[7] H. Torkaman and E. Afjei, "Magnetio Static Field Analysis Regarding the Effects of Dynamic Eccentricity in Switched Reluctance Motor," *Progress in Electromagnetics Research M, PIER,* vol. 8, pp. 163-180, 2009.

[8] H. Torkaman and E. Afjei, "Hybrid Method of Obtaining Degrees of Freedom for Radial Air Gap Length in SRM under Normal and Faulty Conditions Based on Magnetiostatic Model," *Progress In Electromagnetics Research, PIER,* vol. 100, pp. 37-54, 2010.

[9] N. K. Sheth and K. R. Rajagopal, "Effects of Nonuniform Air Gap on the Torque Characteristics of a Switched Reluctance Motor," *IEEE Transactions on Magnetics,* vol. 40, no. 4, pp. 2032-2034, 2004.

[10] N. K. Sheth and K. R. Rajagopal, "Variations in Overall Developed Torque of a Switched Reluctance Motor with Air Gap Nonuniformity," *IEEE Transactions on Magnetics,* vol. 41, no. 10, pp. 3973-3975, 2005.

[11] D. G. Dorrell, I. Chindurza, and C. Cossar, "Effects of Rotor Eccentricity on Torque in Switched Reluctance Machines," *IEEE Transactions on Magnetics,* vol. 41, no. 10, pp. 3961-3963, 2005.

[12] I. Husain, A. Radun, and J. Nairus, "Unbalanced Force Calculation in Switched-Reluctance Machines," *IEEE Transactions on Magnetics,* vol. 36, no. 1, pp. 330-338, 2000.

[13] J. R. Briso-Montiano, R. Karrelmeyer, and E. Dilger, "Simulation of Faults by Means of Finite Element Analysis in a Switched Reluctance Motor," in Multiphysics Conference, pp. 1-6, Frankfurt, 2005.

[14] E. Afjei and H. Torkaman, "The Novel Two Phase Field-Assisted Hybrid SRG: Magnetio Static Field Analysis, Simulation, and Experimental Confirmation," *Progress in Electromagnetics Research B, PIER,* vol. 18, pp. 25-42, 2009.

[15] E. Afjei and H. Torkaman, "Comparison of Two Types of Hybrid Motor/Generator," in 20th International Symposium on Power Electronics, Electrical Drives, Automation and Motion (SPEEDAM), pp. 982-986, Pisa, Italy, 2010.

[16] H. Torkaman and E. Afjei, "Comprehensive Study of 2-D and 3-D Finite Element Analysis of a Switched Reluctance Motor," *Journal of Applied Sciences,* vol. 8, no. 15, pp. 2758-2763, 2008.

[17] H. Torkaman and E. Afjei, "Comprehensive Magnetic Field-Based Study on Effects of Static Rotor Eccentricity in Switched Reluctance Motor Parameters Utilizing Three-Dimensional Finite Element," *Electromagnetics, Taylor and Francis,* vol. 29, no. 5, pp. 421 - 433, 2009.

[18] E. Afjei and H. Torkaman, "Air Gap Eccentricity Fault Diagnosis in Switched Reluctance Motor," in 1st Power Electronic and Drive Systems and Technologies Conference, PEDSTC, Tehran, Iran, 2010, pp. 284-289.

[19] R. Perers, U. Lundin, and M. Leijon, "Saturation Effects on Unbalanced Magnetic Pull in a Hydroelectric Generator With an Eccentric Rotor," *IEEE Transactions on Magnetics,* vol. 43, no. 10, pp. 3884-3890, 2007.

[20] S. Keller, M. T. Xuan, J.-J. Simond, and A. Schwery, "Large Low-Speed Hydro-Generators Unbalanced Magnetic Pulls and Additional Damper Losses in Eccentricity Conditions," *IET Electric Power*

*Applications,* vol. 1, no. 5,  pp. 657 - 664, 2007.

[21] C. Bruzzese, E. Santini, V. Benucci, *et al.*, "Model-Based Eccentricity Diagnosis for a Ship Brushless-Generator Exploiting the Machine Voltage Signature Analysis," in IEEE International Symposium on Diagnostics for Electric Machines, Power Electronics and Drives,  pp. 1-7, 2009.